Lawrence Berkeley National Laboratory
Recent Work

Title
HEAVY ION FUSION HALF-YEAR REPORT, OCTOBER 1, 1982 - MARCH 31, 1983

Permalink
https://escholarship.org/uc/item/3jb5227s

Author
Lawrence Berkeley National Laboratory

Publication Date
1983-04-01

eScholarship.org Powered by the California Digital Library
University of California

LBL-15926
UC-21 c.2

Lawrence Berkeley Laboratory
UNIVERSITY OF CALIFORNIA

Accelerator & Fusion Research Division

RECEIVED
LAWRENCE
BERKELEY LABORATORY
JUN 8 1983
LIBRARY AND
DOCUMENTS SECTION

HEAVY ION FUSION HALF-YEAR REPORT
October 1, 1982 - March 31, 1983

H.I.F. Staff

April 1983

TWO-WEEK LOAN COPY

This is a Library Circulating Copy which may be borrowed for two weeks. For a personal retention copy, call Tech. Info. Division, Ext. 6782.

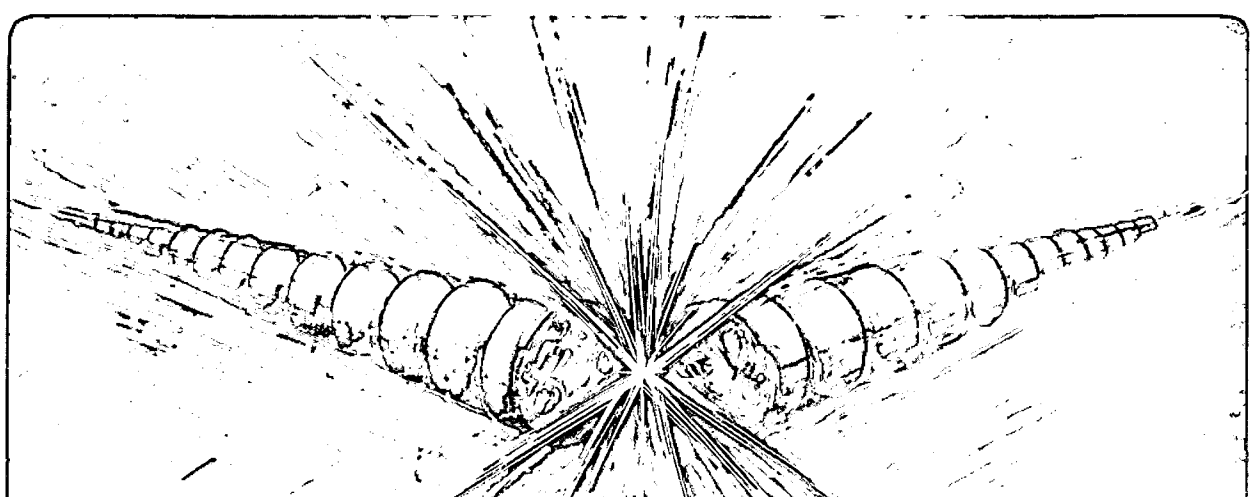

Prepared for the U.S. Department of Energy under Contract DE-AC03-76SF00098

LBL-15926
c.2

DISCLAIMER

This document was prepared as an account of work sponsored by the United States Government. While this document is believed to contain correct information, neither the United States Government nor any agency thereof, nor the Regents of the University of California, nor any of their employees, makes any warranty, express or implied, or assumes any legal responsibility for the accuracy, completeness, or usefulness of any information, apparatus, product, or process disclosed, or represents that its use would not infringe privately owned rights. Reference herein to any specific commercial product, process, or service by its trade name, trademark, manufacturer, or otherwise, does not necessarily constitute or imply its endorsement, recommendation, or favoring by the United States Government or any agency thereof, or the Regents of the University of California. The views and opinions of authors expressed herein do not necessarily state or reflect those of the United States Government or any agency thereof or the Regents of the University of California.

LBL-15926

HEAVY ION FUSION HALF-YEAR REPORT*

October 1, 1982 - March 31, 1983

H.I.F. Staff

April 1983

Lawrence Berkeley Laboratory
University of California
Berkeley, California 94720

*This work was supported by the Assistant Secretary for Defense Programs, Office of Inertial Fusion, Laser Fusion Division, U. S. Dept. of Energy, under Contract No. DE-AC03-76SF00098.

HIGHLIGHTS

The end of this report period has coincided roughly with the IEEE Particle Accelerator Conference at Santa Fe, New Mexico, March 21-23, 1983. It seems appropriate, therefore, that the bulk of this Report be made up of reproductions of four 3-page Conference reports, which give up-to-date analyses and results of four major aspects of the Heavy Ion Fusion Group's activities.

In brief:

- The first acceleration of a heavy ion beam (Cs^{+1}) by a pulsed induction accelerating unit is described in "Long-Pulse Induction Acceleration of Heavy-Ions" by Faltens, Firth, Keefe and Rosenblum. This unit is made up of 12 modules that are separately controlled and can provide ramped voltage pulses of the type needed to initiate beam-current amplification in an ion induction linac for ICF.

- "A Quadrupole Beam Transport Experiment for Heavy Ions Under Extreme Space Charge Conditions" by Chupp, Faltens, Hartwig, Keefe, Kim, Laslett, Nemetz, Pike, Rosenblum, Shiloh, Smith, Tiefenback and Vanecek, describes early results from the single-beam transport experiment. For a single-particle phase-advance per cell (σ_0) less than about 90°, the matched beam transported through five focussing periods has a current density very close to the limiting value set by the cancellation of the restoring force by the space-charge force.

- A new threshold criterion for the longitudinal instability in an intense beam bunch is presented by Bisognano, Smith and Haber, in "Threshold Behavior for Stability of Induction Linac Bunches". Based on both analytic and numerical simulation studies, the instability criterion depends on the beam current, coupling impedance, and bunch length, in relation to the frequency spacing of the potentially unstable modes.

- An ICF scenario using the rf linac and a bunching ring of a novel kind is explored by Selph, Grunder, and Leemann, in "An Isochronous Stacking Ring Approach to the HTE". This is a heavy-ion analogue of the isochronous bunching ring for protons studied by W. Joho for kaon and neutrino experiments. In simplest terms, such a ring avoids the troublesome longitudinal instabilities of conventional storage rings, but at a cost of some other complications that need more detailed study to see if they are of real concern.

LONG-PULSE INDUCTION ACCELERATION OF HEAVY-IONS*

LBL-15119
HI-FAN-216

Andris Faltens, Milton Firth, Denis Keefe, Stephen S. Rosenblum
Lawrence Berkeley Laboratory
University of California
Berkeley, California 94720

Summary

A long-pulse induction acceleration unit has been installed in the high-current Cs^+ beam line at LBL and has accelerated heavy ions. A maximum energy gain of 250 keV for 1.5 μs is possible. The unit comprises 12 independent modules which may be used to synthesize a variety of waveforms by varying the triggering times of the low voltage trigger generators.

Introduction

The Heavy Ion Fusion group at LBL has developed conceptual designs of induction linacs which accelerate a few hundred microcoulombs of charge to megajoule energies for Inertial Confinement Fusion.[1] In these machines a single bunch of ions is accelerated from typically 1 MeV to 10 GeV with an accompanying decrease in pulse duration from about 10 μs at the entrance of the accelerator to 100 ns at the exit (followed by further bunching down to 20 ns in a drift distance between the accelerator and the fusion reactor). Because the ions are nonrelativistic throughout the process and can move with respect to each other, it is necessary to apply longitudinal control to the bunch, in the form of shaped waveforms, in addition to the usual flat voltage pulses (corrected for beam loading) which are required for a monoenergetic output. The required corrections which are new to acceleration of intense beams of heavy ions are, at any instant of time, a linear electric field in space for bunch-length control, plus the negative of the gradient of the space charge potential of the beam for counteracting space charge longitudinal defocusing. These requirements translate into specified desirable applied waveforms at any location. The largest deviations from flat waveforms occur in the low energy portion of the accelerator.

There exists a large technological data-base developed for acceleration of electron beams in the 1-10 kA range[2] which is directly applicable to the greater part of a heavy-ion induction linac. Most of the experience is for pulse durations well under 1 μs, corresponding to the high energy end of the ion accelerator. The large flat-pulse module built at NBS to provide a 2 μs, 400 kV pulse for acceleration of a 1 kA electron beam represents the culmination of an R&D program for economical long pulse modules and provides the only experience base for the low energy end of the ion machine[3]. Here we report on an early stage in an analogous process for heavy ions.

To provide the desired waveforms we are proposing to use a few types of standardized modules, containing core and pulser combinations which can be independently triggered, and to approximate the waveforms in staircase fashion by varying the firing times of a large number of them. The step amplitude chosen in the low energy end of the accelerator is nominally 25 kV, consequently several thousand steps are required with pulse durations longer than 1 μs. While the staircase approximations might appear coarse over a short distance such as 1 meter, they are probably satisfactory when averaged over distances of a few tens of meters (comparable to the bunch length) over which some appreciable intrabunch motion should just start to occur. This distance would contain about 100 modules, a module being defined as a single pulser driving a number of cores (two, in our case).

Description

The first such induction unit has just been completed and installed at the exit of the LBL high-current Cs^+ injector facility,[4] as shown in Figure 1, where it may be used for additional acceleration and correction of the energy profile of the ion beam. The main function of the device, however, is as an engineering prototype of one of the kinds of units that may be required in the future. There are 12 independently driven core pairs, i.e. 12 modules, within a common container, which would increase the particle energy by 250 keV if triggered simultaneously. The typical module consists of a high-power pulse generator which drives two large induction cores in parallel, a reset pulser which restores the magnetic core to negative saturation before the beginning of the acceleration pulse, and a correction network which is used to modify the accelerating pulse. Each core drives two resistively graded sections of the centrally located accelerating column, at a low enough voltage such that each of the two sections can support the full voltage. A simplified sketch of one module and its drive circuitry is shown in Figure 2.

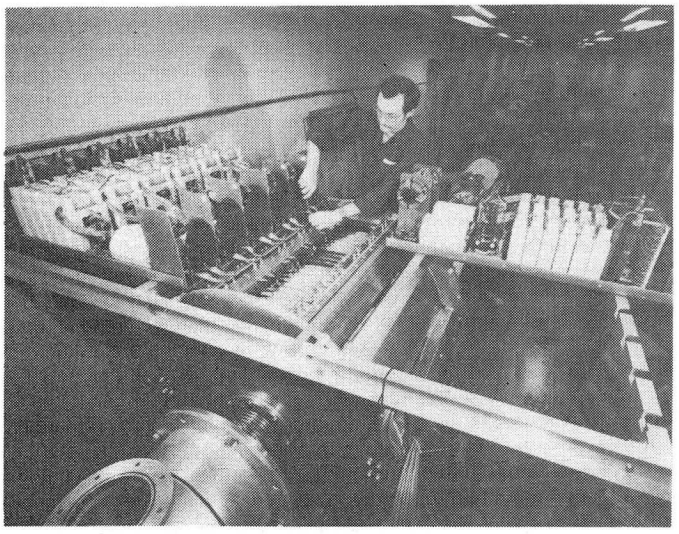

Fig. 1. The induction module being installed in the high-current Cs^+ beam line

The induction core is wound with 2 mil thick 3.25 percent silicon steel tape which is insulated with an inorganic phosphate coating with a ceramic filler, resulting in a radial packing fraction of 92 percent. The cores are insulated axially from the drive conductors with Mylar sheets, and the entire unit is

*Work supported by the Assistant Secretary for Defense Programs, Office of Inertial Fusion, Laser Fusion Division, U.S. Department of Energy, under Contract No. DE-AC03-76SF00098.

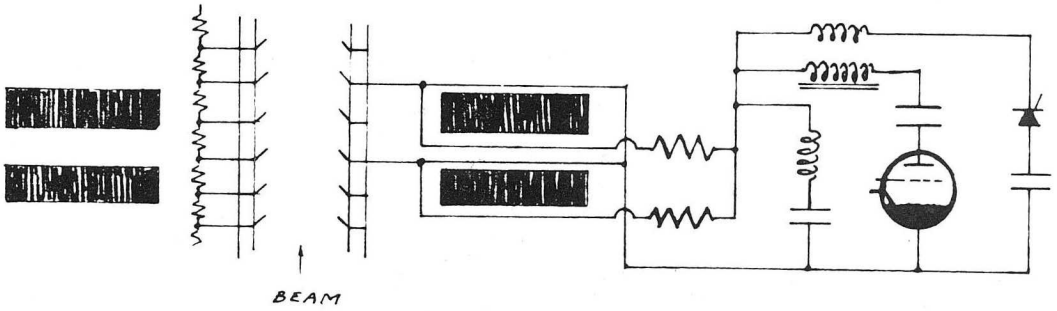

Fig. 2. Simplified sketch of the mechanical arrangement and electrical circuitry for one of the modules of the twelve-section accelerator unit

filled under vacuum with Freon TF, resulting in an axial packing fraction of 75 percent. While the average accelerating field along the column is only 2.5 kV/cm, the fields within the modules occasionally reach 100 kV/cm as a consequence of the dense packing of components within it. The drive conductors are made of copper sheets for the purpose of carrying the heat generated by the core losses to the outer radius with only a few tens of degrees temperature rise at the nominal rep rate of 1 pulse per second. A pulse duration of 1.5 μs was chosen for design purposes although the unit may be used for longer as well as for somewhat shorter pulses.

Results

In the period preceding delivery of the major component parts of the modules, various pulse generator options were tried. Initially, a line type PFN with a total capacity of 1.5 μF was used on a load simulating one core. The final version of this first exercise pulsed more than 2×10^6 times with no signs of degradation. The circuit was then modified to drive a load simulating two parallel cores. With this load the ignitron switching tubes darkened rapidly and failed at 10^5 pulses. Several iterations of the circuit were tried, and the manufacturer of the tube made several modifications to overcome the problems. The present version of the pulse generator uses a saturated inductor in series with the ignitron and a diode across the PFN, which is now essentially a capacitor, to protect the tube from reverse current. With these improvements, a test-module has pulsed in excess of 10^6 times. The gridded ignitron switch which evolved from this work also reduced firing jitter from ± 100 ns to ± 25 ns. A future report will describe the development and performance of the tube.

The completed 12-module unit has recently been placed into service. The oscilloscope traces in Figure 3 show its effect on the transit time of a Cs ion beam through a short drift section after the module. The beam energy at the entrance has been kept low to accentuate the effect. In a larger machine the beam energy would be measured with a spectrometer and the desired voltages applied as here, but the effect of any one unit would be very small. In the near future we will explore the range of available waveforms with the present module, and in the longer term construct a few more prototypes geared more specifically to the requirements of the anticipated High Temperature Experiment.[5, 6]

Design Considerations and Outlook

The choice of an of induction module design depends on the pulse duration and the (usually related) applied voltage. The present design is

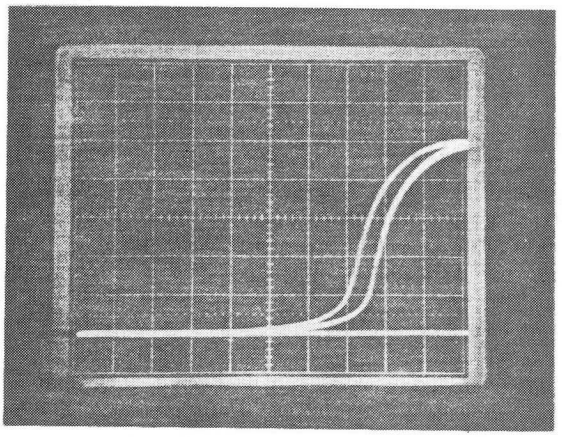

Fig. 3. Difference in times of flight of Cs beam through a 2.5 meter distance after the accelerator unit, for system on and off. Sweep speed 500 ns/div. Four beam pulses at each setting show that the system jitter is less than 50 ns.

suitable for pulses of 1 μs and longer. As the pulse duration is increased the core losses and the electric stresses decrease, while at the same time there is only a small economic incentive to change the design. Going in the other, more difficult direction, however, requires several changes. For shorter pulses, the electric stresses between laminations eventually become excessive, and to reduce them the choices are, first, to decrease lamination width (to a practical minimum of about 1 cm) and second, to decrease lamination thickness (to about 1 mil). For still further reductions in pulse duration, it is necessary to interleave a thin sheet of insulation such as Mylar between the laminations, and, because this form of insulation is much better than the minimum required, it is permissible to increase the tape width. The change to the more positive type of insulation is accompanied by a drop in the radial packing fraction and an increase in winding cost, and it usually precludes annealing the finished core.

A similar change of character occurs in the design of the pulse generating circuitry as the pulse duration is decreased. For pulses greater than 1 μs a lumped element network is satisfactory while for pulses below 100 ns a distributed line is usually preferred for the high-voltage pulses of interest. The present design uses 6 small capacitors to reduce lead inductance and problems with capacitor internal resonances, and the desired waveform is largely achieved with a correction network across the core. If a core is driven from a capacitor, large enough to behave as a voltage source, then the largest use

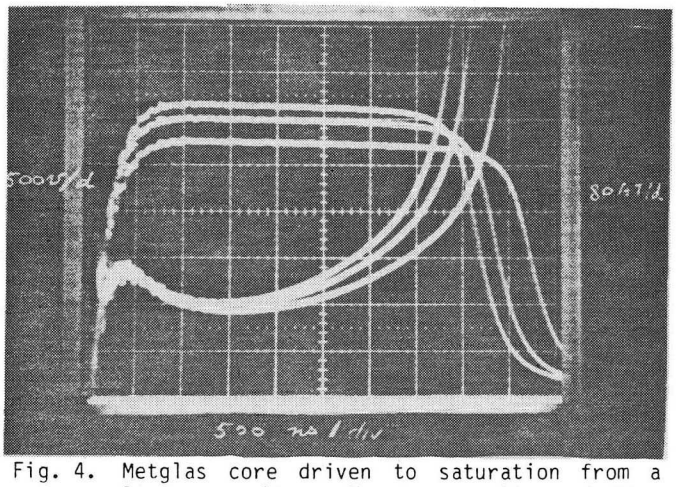

Fig. 4. Metglas core driven to saturation from a large capacitor. Top trace voltage, bottom trace current.

useful flux change can be obtained from the core, but the post-saturation drive current rises to large values, as shown in Figure 4, and efficiency suffers. Ideally, one would like the exciting current to go to zero as the core saturates. While this desirable behavior can be obtained with a controllable switch such as a hard tube, it is too expensive an option. Instead, a simple closing switch, a core with reasonably square-loop behavior, and a pulse-forming network were selected which decrease the post-pulse current at the expense of wasting some of the available flux during the voltage fall time, as shown in Figure 5. The correcting network is essentially an LC across the core which takes energy from the PFN at the start of the pulse, when the drive current is small, and returns it at the end of the pulse when the drive current is large.

The core losses, which are a function of eddy currents and hysteresis, may be reduced by several means, the main one being the use of thinner laminations in the regime of interest for induction linacs. Cost considerations, of course influence the designs. At the time the module was designed, the 2 mil steel was chosen because the pulser cost increased more than the material savings when going to 4 mil steel, and because the material cost increased substantially more than the pulser cost decreased when going to 1 mil material. The recently developed Metglas material, an amorphous magnetic metallic glass tape, has been decreasing in price and might become the material of choice in the future.

While we have been measuring sample cores of Metglas for four years, until recently we have not been able to obtain cores of the size of interest for induction linacs. Now we have two cores of Metglas 2605SC which may be compared, with some adjustment of numbers to take into account dimensional differences, with the silicon steel cores used in the module. Table I below gives the results for the finished cores.

Both types of cores should be considered developmental at this stage, and the costs given are for relatively small quantities of material. The induction change and impedance numbers are approximations for the way in which the cores are used in the present module, and could be improved with both circuit and core developments.

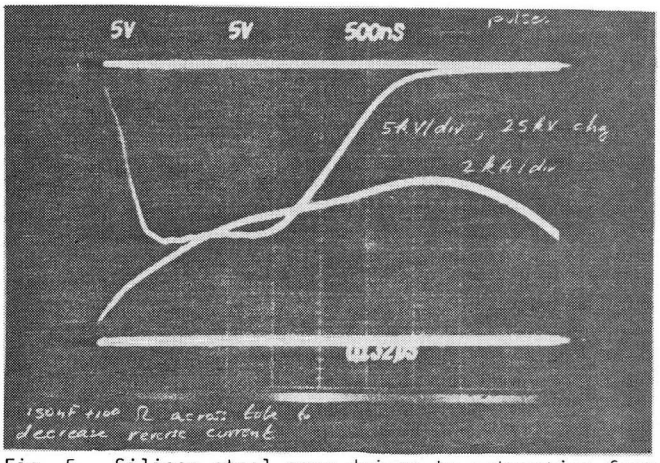

Fig. 5. Silicon steel core driven to saturation from a small capacitor, with a correction network at the output to modify waveform. This is the output voltage from the prototype of one module. Top trace voltage, bottom trace current.

Table I. Comparison of Core Materials

		2 mil silicon steel	Metglas
Saturation Induction,	kG	13.8	10.7
Remanent Induction,	kG	11.4	9.9
Coercive Force	Oe	1	0.1
Available Induction Change at High Impedance,	kG	20	17
Average Apparent Impedance During 1.5μs Pulse	Ω	5	20
Radial Packing Fraction	%	92	75
Cost	$/lb	6	24

Acknowledgment

The authors gratefully acknowledge the support and assistance of Edward Hartwig, Ralph Hipple, August Kruser, Tom Purtell, Jurek Shkredka, Dave Vanecek and the other persons who worked on the construction and installation of the module.

References

1. A. Faltens, E. Hoyer, and D. Keefe, Proc. 4th International Topical Conference on High Power Electron and Ion Beam Research and Technology, (Palaiseau, 1981), H.J. Doucet and J.M. Buzzi (Ecole Ploytechnique, 1981) p. 751.

2. See, for example, the review articles by J.E. Leiss, "Induction Accelerators and their Applications", IEEE Trans on Nuclear Science, NS-26, p. 3870 (1979), and by A. Faltens and D. Keefe, "Review of Induction Linacs", Proc. of the 1981 Linear Accelerator Conf., p. 205, LA-9234-C, October, 1981.

3. J.E. Leiss, N.J. Norris and M.A. Wilson, Particle Accelerators, 10, 223 (1980).

4. W. Chupp, A. Faltens, E. Hartwig, E. Hoyer, D. Keefe, C. Kim, M. Lampel, E. Lofgren, R. Nemetz, S.S. Rosenblum, J. Shiloh, M. Tiefenback and D. Vanecek, IEEE Trans. Nuc. Sci, NS-28, 3389 (1981).

5. R.O. Bangerter, (Compiler) Los Alamos National Laboratory Preprint, LA-UR-81-3830, Dec. 1981.

6. Heavy Ion Fusion Staff, Lawrence Berkeley Laboratory Report PUB-5065 (Feb., 1982).

A QUADRUPOLE BEAM TRANSPORT EXPERIMENT FOR HEAVY IONS UNDER EXTREME SPACE CHARGE CONDITIONS*

LBL-15132
HI-FAN-218

W. Chupp, A. Faltens, E.C. Hartwig, D. Keefe, C.H. Kim, L.J. Laslett,
R. Nemetz, C. Pike, S.S. Rosenblum, J. Shiloh, L. Smith, M. Tiefenback, and D. Vanecek
Lawrence Berkeley Laboratory
University of California
Berkeley, California 94720

Summary

A Cs ion-beam transport experiment is in progress to study beam behavior under extreme space charge conditions. A five-lens section matches the beam into a periodic electrostatic quadrupole FODO channel and its behavior is found to agree with predictions. With the available parameters ($\leq$200 keV, $\leq$20 mA, $\pi\varepsilon_n \geq 10^{-7}$ π rad-m, up to 41 periods) the transverse (betatron) oscillation frequency (ν) can be depressed down to one-tenth of its zero current value (ν_o), where $\nu^2 = \nu_o^2 - \omega_p^2/2$, and ω_p is the beam plasma frequency. The current can be controlled by adjustment of the gun and the emittance can be controlled independently by means of a set of charged grids.

Background

Since Maschke[1] first pointed out that an upper limit on beam current may exist in a quadrupole transport channel, extensive computational studies based on the Kapchinskij-Vladimirskij (K-V) distribution and numerical simulation studies using particle-in-cell (PIC) codes[2] have taken place.

An understanding of how intense beams with high optical quality can be safely transported is of vital importance for the design of an inertial confinement fusion system based on a heavy-ion accelerator driver.[3] Depending on whether the understanding of the transported current limit turns out to be either pessimistic or optimistic, so too will the complexity of the final beam-transport to the fusion target become relieved or further aggravated. In addition, a driver based on linear induction acceleration is best suited to operating near the space-charge limit throughout the length of the device; the design (and cost) of such a driver depends significantly on a knowledge of the transport-limited current.[3]

Some years ago, we proposed a test of the relevant physics using a quasi-dc cesium ion beam with an energy close to 2 MeV -- and a current of 1 ampere[4] passing through a sequence of electromagnetic quadrupoles; for reasons of cost the experiment was abandoned. Instead, the present experiment, which uses a 200 keV Cs^{+1} beam, was instituted and the quadrupoles were chosen to be electrostatic rather than electromagnetic simply because of their lower cost, albeit greater inconvenience. Interest in the same physics has prompted related experiments.[5-7] The classic experiment on Brillouin flow by Brewer is also relevant.[8]

Statement of the Problem

In a quadrupole focussing channel with a single-particle betatron angular frequency ν_o -- corresponding to a phase advance of σ_o per period -- the presence of space charge results in a reduction of the restoring force so that particles have a decreased frequency and phase-advance denoted by ν and σ respectively. (Magnetic and relativistic effects are ignored since the main interest here is for very slow heavy-ion beams.) In the "smooth approximation" the relation between ν and ν_o is given by

$$\nu^2 = \nu_o^2 - \frac{1}{2}\omega_p^2 , \qquad (1)$$

with $\omega_p^2 = \frac{4\pi ne^2}{M}$, the square of the beam plasma frequency, where n is the number of ions per unit volume. (More realistic considerations show that the coefficient 1/2 is not exact, but depends on lattice parameters.) For constant gun voltage, ω_p^2 is directly proportional to the current density, $j = nev$.

Clearly, Eq. 1 predicts that an absolute limit on current density exists when $\nu \to 0$, i.e. $\omega_p \to \sqrt{2}\,\nu_o$, and the net restoring force vanishes. As one nears that limit, the current density remains constant, and as the current is increased the area of the matched beam increases proportionately. Generally, the beam size depends on both the emittance (normalized), $\pi\varepsilon_N$, and the beam current. Absent from the discussion so far, is the prediction of classes of instabilities that cause emittance growth, with consequent beam loss, well before $\omega_p = \sqrt{2}\,\nu_o$. For the case of $\sigma_o \lesssim 60^\circ$ the KV treatment predicts fourth and higher order instabilities below $\sigma = 24^\circ$, but the PIC work indicates no change in rms emittance as σ decreases, at least to $\sigma = 6^\circ$.

The object of the experiment is to explore beam properties after transport, such as size, current, current density (and hence σ/σ_o), over a range of values of σ_o, ε_N, and injected current. The accessible range of parameters should also make the predicted regions of instability amenable to study.

Apparatus

Source

We have operated so far with a thermionic cesium alumino-silicate source (zeolite) 25 mm in diameter. Erratic results over a period of time with commercially available sources were traced to non-uniform coating, non-uniform emission, and departures from flatness in the coating sufficient to interfere with the gun optics. Satisfactory space-charge-limited flow is almost impossible to achieve under these conditions and we have been forced to develop in-house source preparation and testing facilities that have now produced acceptable zeolite sources for both cesium and sodium ions.

Ion Gun

The gun is designed to have a constant output voltage, nominally 200 kV, and variable current density (j = 3 to 6 mA/cm^2), and to operate under space-charge limited conditions. Designed with the help of the EGUN code[9], a four-electrode structure with Pierce geometry proved adequate to provide satisfactory optics over this dynamic range.[10]

*This work was supported by the Assistant Secretary for Defense Programs, Office of Inertial Fusion, Laser Fusion Division, U.S. Department of Energy, under Contract No. DE-AC03-76SF00098.

Attenuators can provide current densities $j < 3$ mA/cm^2. (See Figs. 1 and 2.)

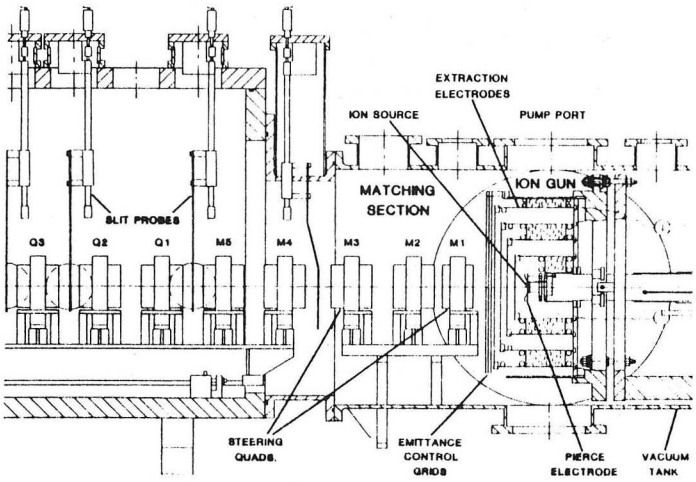

Fig. 1: A drawing of the gun showing emitter with Pierce electrode, separately controlled electrodes, and emittance control grid.

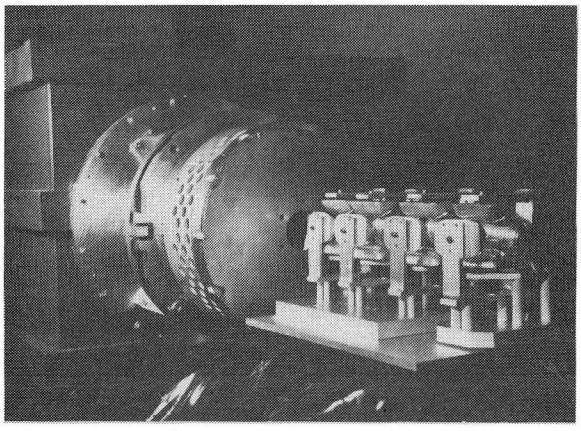

Fig. 2: The gun with four matching quadrupoles in place.

Beam Transport Quadrupoles

When completed, the transport channel will consist of 82 electrostatic quadrupoles -- 41 periods of a FODO lattice -- housed in a sequence of seven vacuum chambers. At present, just one chamber containing the initial 10 quadrupoles (Q1 - Q10) is in place; the others will be added sequentially as dictated by the progress of experimental understanding. Five quadrupoles (M1 - M5), placed between the gun and the transport system and independently controlled, form the matching section to transform the axially-symmetric transverse phase areas at the gun output into the astigmatic phase ellipses needed at the entry into the transport section.

The design of an experiment to test long-term stability in any quadrupole channel, for conditions where the net restoring force can become very small, is especially demanding. Since one is seeking to detect the threshold at which deterioration in beam quality occurs due to collective instabilities, it is important that damaging effects, such as could arise from non-linearities that affect single-particle motion, be avoided. In designing the system of electrostatic quadrupoles, one of us (L.J.L.)[11] developed 3-D relaxation codes to compute the electric fields for a large variety of electrode shapes, and particle dynamics codes based on the K-V distribution to predict the beam behavior, taking into account non-conservation of particle kinetic energy, asymmetric images, and non-paraxial effects. An additional feature of his work was the development of acceptable electrode shapes that could be very simply machined.

The final configuration chosen had a FODO period of 12", a physical aperture radius of 1", and an inter-lens gap of 2.0", Figure 3 shows the first of the seven transport vacuum tanks in place; as can be seen, a liberal allotment of penetrations has been provided for possible introduction of frequent diagnostic devices.

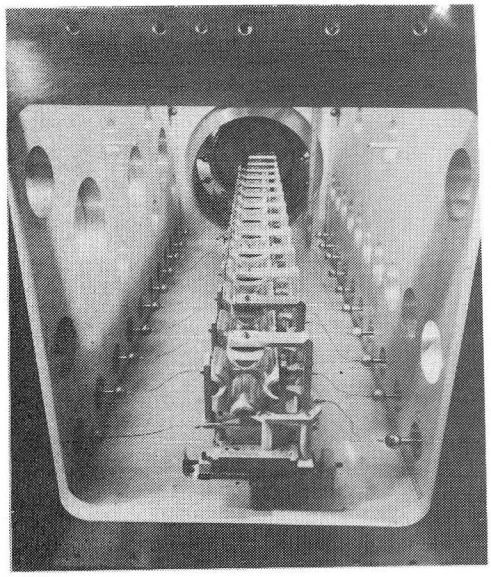

Fig. 3: View (towards gun) of transport and matching quadrupoles.

Beam-conditioning and Diagnostic Devices

Apart from complicating the study of beam-dynamics, electrostatic lenses also impose constraints and difficulties on the incorporation of diagnostics. Measurement devices can be inserted only at the mid-point of the free-space between adjacent lenses, i.e. where there is a ground equipotential, and are constrained to be thin to avoid sparking. Electron production by ions striking material surfaces may also cause some problems.

Beam-conditioning devices include: (a) a grid-structure after the gun to which voltages can be applied to alter the emittance over the range $\varepsilon_N = 1\times10^{-7}$ rad-m to 1×10^{-6} rad-m; (b) attenuator grids after the gun; (c) a collimator after the gun to select a 3 mm diameter attenuated pencil beam. On axis, this provides a beam in which the behavior is dominated by emittance, not space-charge. Off-axis, it provides a tool for checking the single-particle tune, σ_o, of the transport system.

Diagnostics include: (i) slim Faraday cups with bias grids to measure beam current; (ii) metal plates with slits which can be moved across the beam upstream of a Faraday cup. Scanning with a single slit determines the projected beam profile. Setting one slit at a sequence of locations and scanning with a second slit downstream allows the beam emittance to be mapped in either plane; (iii) transparent scintillators that can be moved into the

beam and the light recorded by a gated photo-diode camera.

Experimental Procedure

In principle, the computer-assisted procedure for arriving at a matched beam throughout the transport section is straightforward. The gun electrodes are set to voltages calculated from EGUN to provide the chosen beam current and gun optics. The emittances in the x and y-planes -- described by a set $\rho = (r_x, \theta_x, r_y, \theta_y)$ -- are measured at the gun exit. The EQENV code provides the x and y emittance ellipse shapes and orientations that are needed at the entrance of the FODO transport structure to establish the matched beam condition for the chosen values of current and σ_0. A related code, PARAX, is then used to derive the voltages, V_i, needed on the matching quadrupoles to transform the ellipses fitted from observations at the gun exit, ρ_G, into the matched ellipses, ρ_M, after the matching section where they can be checked experimentally. If the measurements do not conform to expectation with an error $\delta\rho$, a computer-constructed linear response matrix, A_{ij}, provides the set of voltage corrections, $\delta V_i = A_{ij}\ \delta\rho_j$, to move towards the correct solution. A further similar iteration can be applied if needed. A necessary check, of course, lies in the measurement of the emittance, ρ_T, at the end of the transport section (at present 5 periods long) to establish that $\rho_T = \rho_M$, and in checking that no beam has been lost along the way.

In practice, the success of this method proved highly sensitive to source imperfections such as spotty emission, misalignment, time variation, etc., which can spoil the adequacy of first order corrections and cause the procedure to fail to converge. With the recent inhouse development of more stable and uniform sources, the procedure has been found to work well, converging to an acceptable value with a single linear correction.

Experimental Results

Figure 4 displays some sample results for a single choice of beam current, I_b = 11 mA, and a single choice of emittance, $\varepsilon_N \approx 1\text{x}10^{-7}$ rad-meters, for the present set-up with the five matching quadrupoles, followed by five periods of the FODO transport section. The matching procedure described above worked well for $\sigma_0 < 100°$, in the sense that the appropriate beam sizes and emittance ellipse tilts could be attained within 10 percent at both the entrance and the end of the transport section (Q1 - Q10). At large values of σ_0 some of the calculations indicate beam-envelope sizes that become either large or small in the matching section and the procedure is less reliable. Also, the KV calculations indicate that for 11 mA a strong envelope instability should be present near 120°.

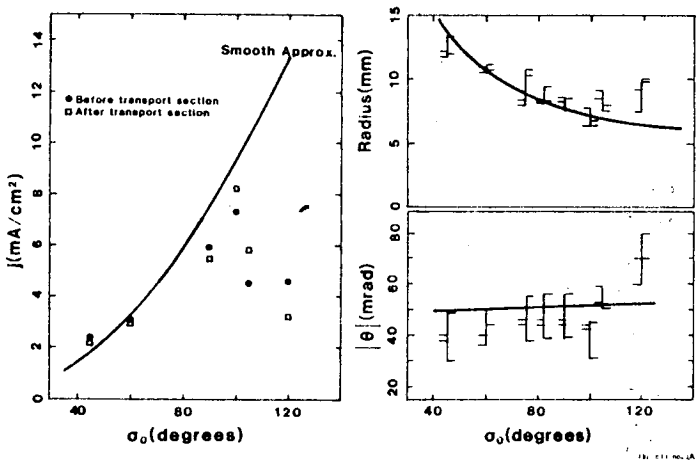

Fig. 4: Measured current density, beam radius, and envelope divergence (curves are calculated matched values).

If there is a mismatch the beam area measured at the exit of Q10 may be larger or smaller than the matched value, depending on the phase of the envelope oscillations at that point. This, apart from some uncertainties in the Faraday cup calibrations, leads to errors in the estimates of j. Thus the scatter in the data points for beam size and j in Fig. 4 are seen to be anti-correlated.

If we denote a limiting current density, corresponding to $\omega_p = \sqrt{2}\ \nu_0$, by j_L, the data indicate transport (over 5 periods) of $j \approx j_L$ for $\sigma_0 \lesssim 100°$. The corresponding value of $\sigma/\sigma_0 = (1-j/j_L)^{1/2}$ is poorly determined but is probably in the range of 0.1 to 0.3.

The large dimensionality of the experiment is illustrated by the fact that only a small part of the transport section is being studied and that a range of values of both I_b and ε_N remains to be explored.

References

1. A.W. Maschke, Brookhaven Nat'l Lab. Rep., BNL-20297 (1975).
2. For refs. see: L. Smith, Proc. 1981 Lin. Acc. Conf., Los Alamos Report LA-9234-C, 111 (1982).
3. For refs. see: D. Keefe, Ann. Rev. Nuc. Part. Sci., 32, 391 (1982).
4. D. Keefe, Proc. Heavy Ion Fus. Workshop, BNL-50796, 4 (1977).
5. J.D.Lawson, et al., elsewhere in these Proceedings.
6. J. Klabunde, et al., ibid.
7. A.W. Maschke, et al., ibid.
8. G.R. Brewer, Jour. App. Phys., 30, 1022 (1959).
9. W.B. Herrmannsfeldt, Stanford Linear Accelerator Center Report SLAC 226, (1979).
10. C. Kim, Lawrence Berkeley Laboratory Internal Report, HIFAN-160 (1981).
11. L.J. Laslett, Lawrence Berkeley Laboratory Internal Reports, LBID-244 (1980), HIFAN-106 (1980), HIFAN-137 (1980), HIFAN-150, 150A (1981).

THRESHOLD BEHAVIOR FOR LONGITUDINAL STABILITY OF INDUCTION LINAC BUNCHES*

J. Bisognano, I. Haber†, L. Smith
Lawrence Berkeley Laboratory
University of California
Berkeley, California 94720

Summary

The induction linac bunches of heavy ion fusion scenarios are strongly influenced by the longitudinal space charge impedance. This is in distinct contrast to relativistic bunches in storage rings where most of the data on stability have been obtained. Simulation results reveal that when space charge effects are large, the stability requirement of small growth rate relative to the synchrotron frequency for relativistic bunches is replaced by the relaxed condition of small growth rate relative to the frequency spacing of the space charge wave modes on the bunch. Dispersive effects from finite pipe size tend to make the lower frequencies less susceptible to instability than higher frequencies. Since induction modules have a high resistive component only for the lowest bunch modes, stability is better than would occur for a broadband impedance of comparable magnitude. These results indicate that long term longitudinal bunch stability is realizable for induction linac drivers for heavy ion fusion.

Introduction

The final lens system for focusing an intense beam of heavy ions for inertial confinement fusion requires a very small longitudinal velocity spread. For a uniform beam the currents envisioned would be above threshold for longitudinal instability driven by the induction module and space charge impedance, and would contribute to growth of the velocity spread. For bunched beams, however, there is clear evidence[1,2] that the coupling of growing waves and damping waves through bunch end reflections can have a stabilizing influence. However, for sufficiently fast growth rates it has been observed in relativistic storage rings that this reflection mechanism breaks down. These issues have been addressed through a particle simulation code[3] which can model an arbitrary machine impedance including space charge forces (with finite pipe size effects) in an induction linear accelerator. Results indicate that the end reflection process does indeed improve the long term stability characteristics of an induction linac bunched beam. Ultimately, an instability threshold is reached, but at values of the module impedance which are higher than required for typical induction linac drivers. Dispersive effects introduced by the finite pipe size reduce the group velocity of high frequency perturbations, making their threshold requirements more severe. The thresholds observed are consistent with a mode coupling model of the bunch instability analogous to Sacherer's[4] analysis of storage ring bunch instabilities.

Coherent Longitudinal Bunch Dynamics

The coherent propagation of a longitudinal perturbation on an induction linac bunch is driven by the induction module impedance and space charge. The impedance of the induction module is well represented over the most important frequency range by a parallel RLC circuit. The dispersive space charge force law of a beam in a circular pipe can be approximated by an electric field whose k dependence is given by

$$E \propto \frac{ik}{1 + \alpha k^2} \tag{1}$$

where $\alpha = (B/2.4)^2$ for pipe radius B. This expression is obtained from a Bessel function expansion of the longitudinal field in a finite pipe, with the value 2.4 the first zero of J_0. For a purely rectangular, cold bunch of length L, space charge wave modes can be obtained from a fluid model. The eigenfrequencies of these modes are given by

$$\omega_n^2 = v_o^2 (k_n)^2/(1 + \alpha k_n^2) \tag{2}$$

$$k_n = \frac{\pi n}{L} \tag{3}$$

where n is any integer and L is the bunch length. The plasma wave velocity, V_o, is given by

$$v_o^2 = q^2 g\lambda/m \quad , \tag{4}$$

for charge q, $g = 1 + 2Ln\ (B/A)$, line density (λ) beam radius A, and mass m. Note that at high frequencies the modes coalesce, and the group velocity tends to zero.

Microwave Instability

For a non-relativistic uniform beam the threshold for longitudinal instability for machine impedance per unit length Z' and wave vector k is given by the Landau damping[5] condition

$$v_o^2(Z'v/k) > 2\pi F\ v_{th}^2 \tag{5}$$

where v_{th} is the full width, half height velocity spread, v is the beam velocity, and F is a form factor of the order of unity.

For relativistic bunched beams in a storage ring it has been found that if the analogous condition is satisfied for modes of wavelengths shorter than the bunch, there is instability only if the associated growth rate exceeds the synchrotron angular frequency. Sacherer[4] has analyzed this phenomenon in terms of a perturbation expansion, and found that the above condition corresponds to strong coupling of the unperturbed modes of the bunch by the machine impedance Z'. The coupling is strong if the associated growth rate exceeds the local mode spacing. For hot bunches, where the thermal velocity greatly exceeds the plasma wave velocity, the mode spacing is the synchrotron angular frequency.

Simulations of the hot bunch microwave instability were performed, with the machine impedance modeled with the usual Q = 1 resonator which has been found to well represent most storage rings. A threshold for instability was found with the above form factor

*This work was supported by the Director, Office of Energy Research, Office of High Energy and Nuclear Physics, High Energy Physics Division, U. S. Dept. of Energy, under Contract No. DE-AC03-76SF00098.

†Naval Research Laboratory, Washington, D.C. 20375

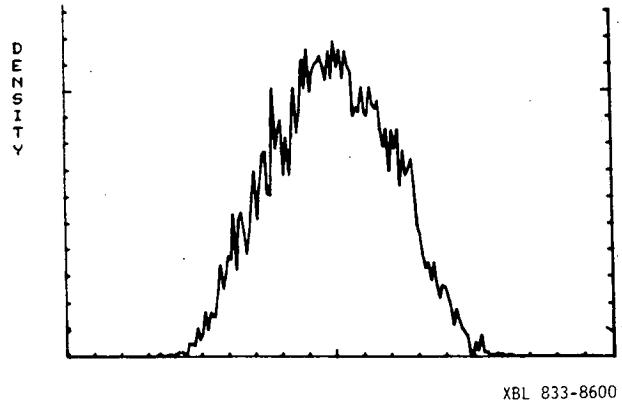

Figure 1: Equilibrium longitudinal density of an initially parabolic distribution below microwave instability threshold.

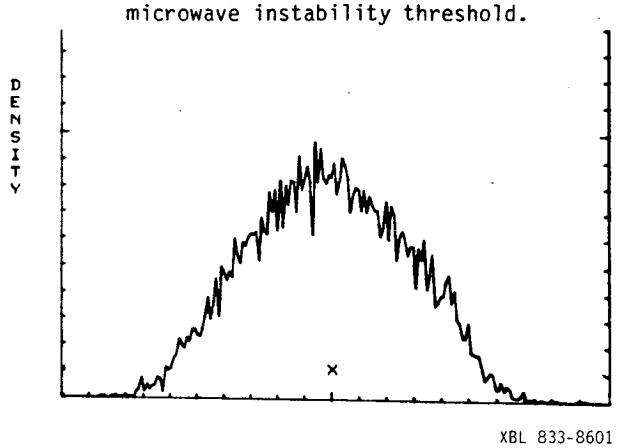

Figure 2: Equilibrium longitudinal density of an initially parabolic distribution above microwave instability threshold.

F = 0.6. Figures 1 and 2 show the density distribution after saturation of a parabolic bunch below and above the stability threshold, respectively. The initial velocity spread and bunch length were the same in both cases, with the impedance doubled in the latter to exceed the instability threshold. Below threshold, there has been some softening of the sharp edged parabolic distribution, but no appreciable bunch lengthening. Above threshold, the bunch lengthens until an equilibrium is reached.

Instability Thresholds for Induction Linac Bunches

In the simulations shown, induction linac bunches are modeled by a uniform density with 10% parabolic ends. The thermal spread was constant over the uniform region with a value of approximately 0.1 of the wave velocity v_0. In the parabolic ends the phase space distribution is elliptic.[6] The beam pipe radius is .05 of the bunch length. Figure 3 illustrates the resulting phase space distribution. Runs were performed using a resistance with a high frequency rolloff. The magnitude of the resistance is best expressed in terms of e-folding lengths L_e of the nondispersive uniform beam longitudinal instability. The e-folding length is inversely proportional to the resistance in the parameter regime studied. Figures 4, 5, 6 are phase space plots of runs with resistive e-folding lengths of 0.6, 0.3, 0.15 bunch lengths and at times corresponding to 12, 6, and 3 plasma wave traversals along the bunch. Thus, each figure represents the same total

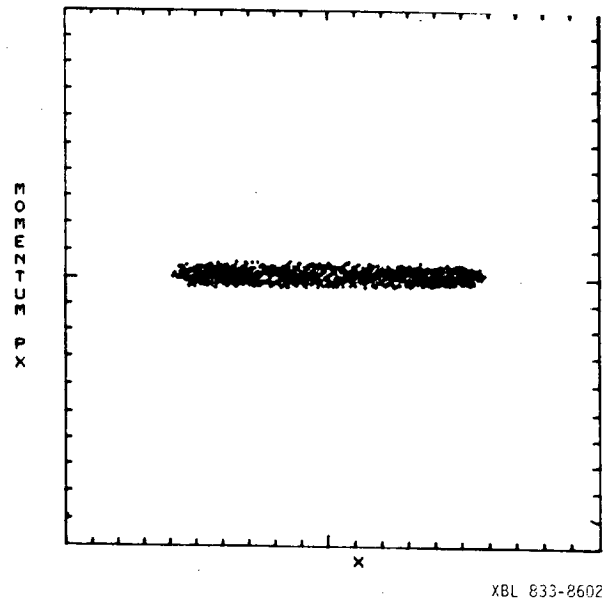

Figure 3: Initial phase space distribution for a model induction linac bunch.

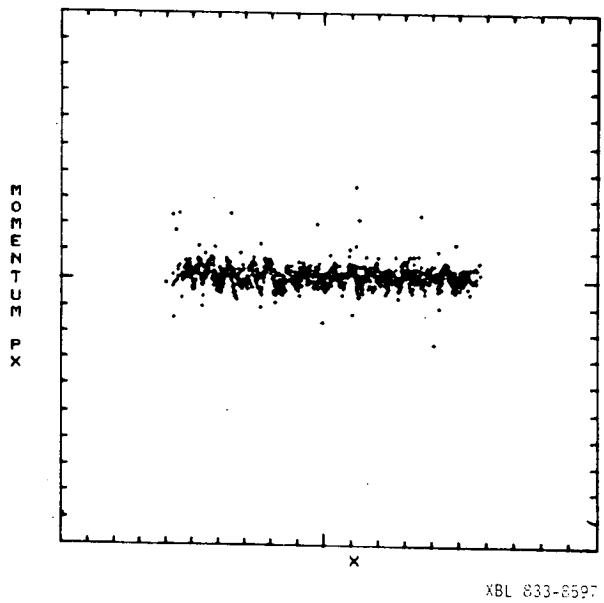

Figure 4: Phase space distribution for L_e = .6 after 12 plasma wave traversals.

exponential growth if there is no reflection stabilization. (All cases are well above the Landau damping threshold as determined primarily by the space charge force, which is unchanged from case to case.) It is clear that a threshold for instability has been crossed. A calculation of the ratio of the uniform beam growth rate γ to the spacing $\Delta\omega_n$ of the modes of Eq. (2) is shown in Table 1, and suggests a criterion similar to that of Sacherer's. The higher frequency modes are more closely spaced because of the space charge dispersion, and low frequencies should be relatively less susceptible to instability. This appears to be borne out in that low frequency growth is more dominant for the shortest e-folding length.

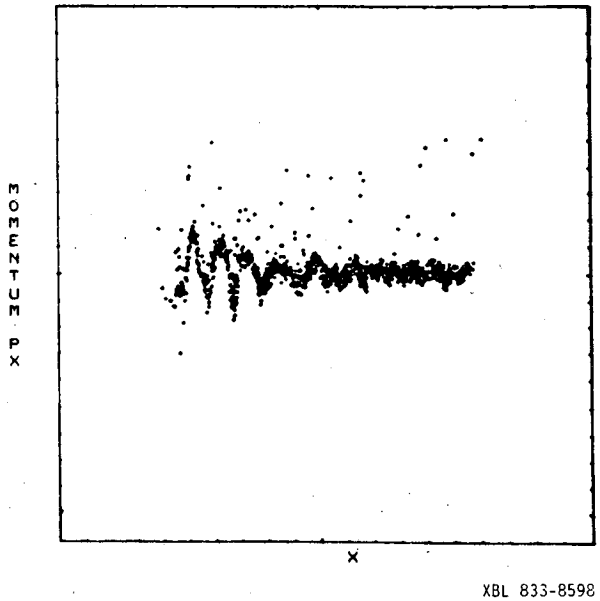

XBL 833-8598

Figure 5: Phase space distribution for L_e = .3 after 6 plasma wave traversals.

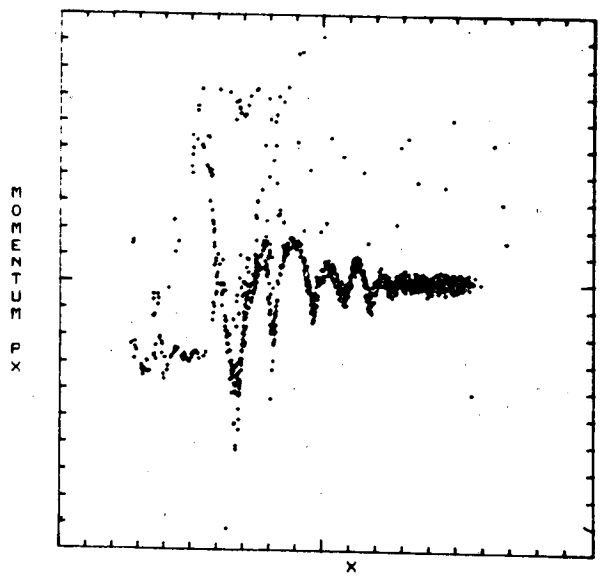

XBL 833-8596

Figure 6: Phase space distribution for L_e = .15 after 3 plasma wave traversals

Table 1
Uniform Growth Rate/Mode $\Delta\omega_n$ Spacing

Mode Number	e-folding length =	.6	.3	.15
2		.65	1.3	2.6
6		.65	1.3	2.6
10		.70	1.4	2.8
14		.75	1.5	3.0
18		.85	1.7	3.4

It should be noted that the above criterion corresponds to a calculation of the e-folding length using the group velocity and comparing the values obtained to the bunch length. The mode spacing provides the proportionality constant.

Several runs were made to explore this threshold phenomenon and the conjecture that instability occurs only if the ratio $S = \gamma/\Delta\omega_n$ is of the order unity or greater. Increasing the bunch length reduces the spacing of modes and increases S. It was found that doubling the bunch length for L_e = 0.6 does indeed induce instability, with a time-scaled growth comparable to the short bunch, L_e = 0.3 case. As another test of the criterion, a narrowband impedance was investigated, with peak values corresponding to the fifth and fifteenth mode. Because of the space charge dispersion, it was possible to choose a single value for the peak impedance such that for mode 5, S < 1.3, and for mode 15, S > 2. The lower S valued case was stable, whereas the higher was found to be unstable. When the dispersion was enhanced by increasing α, the fifth harmonic could be driven unstable, with again S > 2.

Stability Requirements for HIF Induction Linacs

The impedance of HIF induction modules is large at low frequencies, with a frequency halfwidth corresponding to only several harmonics on the bunch. It is at these frequencies that dispersive effects are at a minimum and, therefore, stability is at a maximum. Runs modeling the induction module impedance exhibit stability for growth lengths of 0.3 bunch lengths (calculated from the peak module resistance).

These results indicate that module impedances of several hundred ohms/meter, which provide good linac efficiency, can be tolerated for a variety of induction linac driver parameters. Since the threshold value of Z' scales inversely with bunch length, short bunches are to be preferred from the point of view of longitudinal stability. The numerical studies presented are strictly applicable to single beam transport, and include neither acceleration nor multiple beam interactions. Matching of the end longitudinal focusing has been idealized. These issues may be of importance in determining stability thresholds and beam quality, and are currently being explored.

In conclusion, numerical results suggest that long term longitudinal stability is realizable for induction linac HIF drivers. The magnitude of the longitudinal machine impedance cannot be disregarded in obtaining an optimal design, but there is sufficient flexibility in the choice of machine parameters to permit both high linac efficiency and long term longitudinal beam stability.

References

1. F.J. Sacherer, IEEE Trans. on Nucl. Sci., Vol. NS-22, No. 3, p. 825 (1973)

2. J.M. Wang and C. Pellegrini, Proceedings of the International Conference on High Energy Accelerators, Geneva, p. 554 (1980).

3. J. Bisognano, I. Haber, L. Smith, and A. Sternlieb, IEEE Trans. on Nucl. Sci., Vol. NS-28, No. 3, p. 2513 (1981).

4. F.J. Sacherer, IEEE Trans. on Nucl. Sci., Vol. NS-24, No. 3, p. 1393 (1977).

5. D. Neuffer, Particle Accelerators, 11, 1, p. 23 (1980).

AN ISOCHRONOUS STACKING RING APPROACH TO THE HTE*

LBL-15208
HI-FAN-219

F. Selph, H. Grunder and B. Leemann
Lawrence Berkeley Laboratory
University of California
Berkeley, CA 94720

Introduction

The problem of finding a suitable apparatus for demonstrating heavy ion fusion is a difficult one to approach in moderate steps. An accelerator which can achieve break-even is probably too expensive as a first step in the present climate of trimmed budgets. As suggested by Mark et. al.[1] a meaningful test of many of the concepts could be achieved with a device capable of heating a disk of material to plasma temperatures in the neighborhood of 100 eV (10^6 degrees K). Such apparatus would be useful for testing beam transport, focusing and targeting concepts, as well as target behavior in the plasma regime. Ideally, the technology used in this "high temperature experiment" (HTE) could also be extended to construct a prototype fusion facility.

Target heating for the HTE requires a short beam burst on the order of tens of nanoseconds with a total beam energy of a kilojoule or more. The rf linac falls far short of this capability. A number of studies have considered the use of storage rings for accumulating beam current. The present paper looks at an alternative means, using a rf linac followed by an isochronous stacking ring (ISR), producing rapidly the high multiplication of beam current required. This method avoids the necessity for beam manipulations such as beam splitting, rf bunching in a storage ring, etc. Because of the fast transit time in the ISR, storage ring instabilities are not a problem.

Beam Stacking with an Isochronous Ring

In an isochronous ring, the effective magnetic radius R will be proportional to momentum, and from this we deduce that the radial separation of adjacent orbits is given by (non-relativistically)

$$\Delta R = \frac{2\pi qV\bar{R}}{T_n A \cdot 2} \qquad (1)$$

where V is the accelerating voltage per turn, q is the charge state, A is the mass number, and T_n is energy per nucleon. For injection into the inner radius of the ring, ΔR must be made large enough so that turn separation will be sufficient for beam to clear the septum. At larger radii V can be decreased, even reduced to zero at extraction radius, causing a large number of turns to occupy a small radial extent.

The use of this property of turn-compression, to stack a large current of protons in an isochronous ring at extraction radius, has been studied by Joho[2]. By assuming conservation of longitudinal phase space, he finds that N_m, the maximum number of turns which can be stacked is related to the energy spread ΔT_o of the extracted beam by the formula

$$N_m = \frac{\Delta\Psi_o}{\Delta\Psi_i} \quad \frac{\Delta T_o}{E_{g,i}} \quad , \qquad (2)$$

where $\Delta\Psi$, $\Delta\Psi_o$ are the phase spreads at injection and extraction, respectively, and $E_{g,i}$ is the energy gain per turn at injection. From Eq. 2 we see that to achieve a large number of stacked turns both the phase spread at injection and the energy gain per turn at injection should be as small as possible. The energy spread at extraction should be as large as is consistent with transport to the target.

The maximum current which can be stacked near the outer radius will be limited by the incoherent betatron tune shift. The space charge forces act to shift ν_r, ν_z downward. Thus locating ν_r and ν_z well above integral stopbands is an important consideration in order to maximize allowable current. In order to lower the required energy gain per turn at injection, ν_r is set to 1.25. Then by injecting on a displaced orbit, a coherent betatron oscillation can be produced which will aid the beam in clearing the septum, so the energy gain per turn at injection can be made on-third as large as would otherwise be necessary.

A computer program has been written to track particles through an ISR, in a simulation of the stacking process. Space charge effects have not as yet been included in these calculations. Fig. 1 shows the accelerating voltage used for the particular case which will be illustrated in this paper. Fig. 2 shows the particle energy, the rms energy spread and phase spread of the last 100 turns, as a function of the turn number. This demonstrates the compression, which is optimum at 320 turns in this case, as well as the corresponding phase growth. Particles would be extracted where ΔT_{rms} is a minimum, but the calculation has been extended further, showing an increase in both ΔT_{rms} and $\Delta\Psi_{rms}$. The reason for this behavior becomes clearer in Fig. 3, where the ΔT, $\Delta\Psi$ phase space boundary of a group of particles is plotted at injection, at minimum ΔT_{rms}, and at a later time. It is evident that as the phase space is compressed in energy, the corresponding extension in phase results in particles with a phase shift obtaining less energy, thus distorting the phase space.

Use of an ISR for the HTE

In Fig. 4 is shown the elements of the proposed HTE using an isochronous ring. The apparatus consists of an ion source, a rf linac, a stacking ring and a number of beam lines to transfer beam bunches to the target. By operating the ring on a suitable harmonic, the beam bunch structure is retained, with bunch separations such that fast kicker magnets can be used for extraction and switching in the external beam lines. After extraction, a separate beam line is used for each bunch. Bunch length, which has been established by the choice of rf frequency, is made to be consistent with the pulse length needed for the test.

The beam bunches are formed at the entrance to the linac by a low beta structure, operated a low rf frequency, on the order of 5-10 MHz. As the ions proceed through the linac, the rf frequency is progressivly raised, so that at the exit the frequency is on the order of 50-100 MHz. In the

*This work was supported by the Director, Office of Energy Research, Office of High Energy and Nuclear Physics, Nuclear Science Division, U.S. Dept. of Energy under Contract No. DE-AC03-76SF00098.

present example, the beam energy on target required is about 5 MeV/A, of this the linac will provide 4.55 MeV/A, the isochronous ring the remainder.

Although in the present paper no attempt has been made to estimate costs, we can recognize here a few of the considerations that must be taken into account in optimizing this system.

- In order to reduce the number of beam lines to the target, the circumference of the ISR should be made as small as possible. Thus we consider superconducting magnets as being most desirable.
- To obtain the maximum stacked current it is necessary to use q=1, with A as large as economy permits, because the ring space charge limit is proportional to A/q^2.
- Choosing a low injection energy in the ring will lower the linac cost, but there is practical limit imposed by the width of the field in the ring dipoles. As the field width is increased, the magnet cost will go up. Thus the ring injection energy will probably be determined by minimizing the overall cost of linac + ring.

Target Requirements

We must know the requirements for the HTE target conditions to be achieved in order to design a suitable accelerator. The most important considerations are - the target temperature T reached for a given irradiance S (in Watts/cm^2) as a function of time, the requirements for beam transport, and for focusing on the target.

The maximum divergence and momentum spread are set by the permissible aberrations in the final transport elements. This problem has been discussed in several papers[3]. For this study we will use for maximum divergence, ± 30 mrad, with momentum spread ± 0.25 percent.

As the temperature of a material is raised, energy is deposited in internal degrees of freedom, until such time as electron bonds are broken and the material begins to disassociate. Using as a model a disk of low-density material imbedded in the surface of high-density material, this behavior has been studied with the aid of computer simulations[1,4]. An empirical formula which represents these results to a good approximation is [5]

$$t/\tau = \int_0^x \frac{x^{1/2}}{1-x^4}\,dx \qquad (3)$$

where $x = T/T_f$, with T_f defined by $S = \sigma T_f^4$ and

$$\tau = \frac{3C_1 R}{2\sigma T_f^{5/2}} \qquad (4)$$

The "heat coefficient" $C_1 = 1.02\ 10^4$ J/(gm-eV$^{3/2}$), the ion range R is assumed to be 10 mg/cm^2, and σ is the Stefan-Boltzmann constant, $1.03\ 10^5$ W/(cm^2-eV^4). Eq. 3 is plotted in Fig. 5. We note that as T approaches the asymptotic limit T_f the material starts to disassociate. To determine a useful pulse length we will take $t = \tau$, where $T = 0.95\ T_f$, and presumably the blowing-up process has just started. A longer pulse than τ would waste particles because the last arrivals would not contribute to raising the temperature, while for a shorter pulse than τ, T would fall short of $0.95\ T_f$.

Ring and Target Parameters

There is no unique choice of parameters to reach a given target temperature. The higher the mass number A, the easier it will be to reach a given temperature, but increasing A increases the cost of linac, ring, and transport lines. In the limits of the present paper we cannot treat this subject more fully, instead will use a set of parameters chosen to demonstrate the possibility of using an isochronous ring to achieve a temperature high enough to be useful for the HTE. Ring and target parameters based upon this choice are given in Table I. The stacking behavior has been illustrated in Figs. 1-3.

Table I. HTE Parameters Using A=165, q=1+

Ion Source	Current	7	mA
	Emittance (norm.)	0.3π	mm-mrad
Linac	Low β rf freq.	5	MHz
	Final rf freq.	50	MHz
	" energy	4.55	MeV/A
	" emittance (norm.)	$1.0\ \pi$	mm-mrad
	Momentum spread	$\pm 0.25 \cdot 10^{-4}$	
Ring	Energy at extraction	5.0	MeV/A
	RF frequency	10.0	MHz
	No. of beam bunches	19	
	Ions per bunch	$9 \cdot 10^{11}$	
	Dipole magnet field	6	Tesla
	Accelerating field at injection	0.74	MV/turn
	Betatron frequencies ν_r, ν_z	1.25, 0.9	
	No. of stacked turns	100	
	Transit time in ring	1.6	msec
Target	Spot radius	1.0	mm
	Total no. of particles	$1.7 \cdot 10^{13}$	
	Ion range	10	mg/cm^2
	Pulse length	50	nsec
	Irradiation	$1.5 \cdot 10^{12}$	W/cm^2
	Total energy	2.2	kJ
	Disk temperature	59	eV

Conculsions

There is a strong possibility that isochronous stacking rings will be a useful tool for producing the intense bursts of heavy ions needed for the HTE. Also, it appears that this technology can be extrapolated for use in a heavy ion fusion driver. Additional work needs to be done on the effects of the stacking process on phase space dilution, particularly the effect of space charge. The design of suitable large-aperature superconducting magnets also needs to be studied.

Acknowledgements

We are indebted to D. Judd and L. Smith for valuable suggestions on the dynamics of isochronous rings. S. Boyle has been very helpful with computer software.

References

1. J. Mark, Proc. of the Symposium on Accelerator Aspects of Heavy Ion Fusion, Darmstadt, 1982 (GSI-82-8), pp. 454-513.
2. W. Joho, SIN unpublished report, April 1982, and Particle Accelerators 6, pp. 41-52 (1974).
3. Proceeding of Darmstadt Symposium (see ref. 1, pp. 362-402). See also report of earlier HIF workshops.
4. R. Bangerter, private communication.
5. E. Lee, private communication.

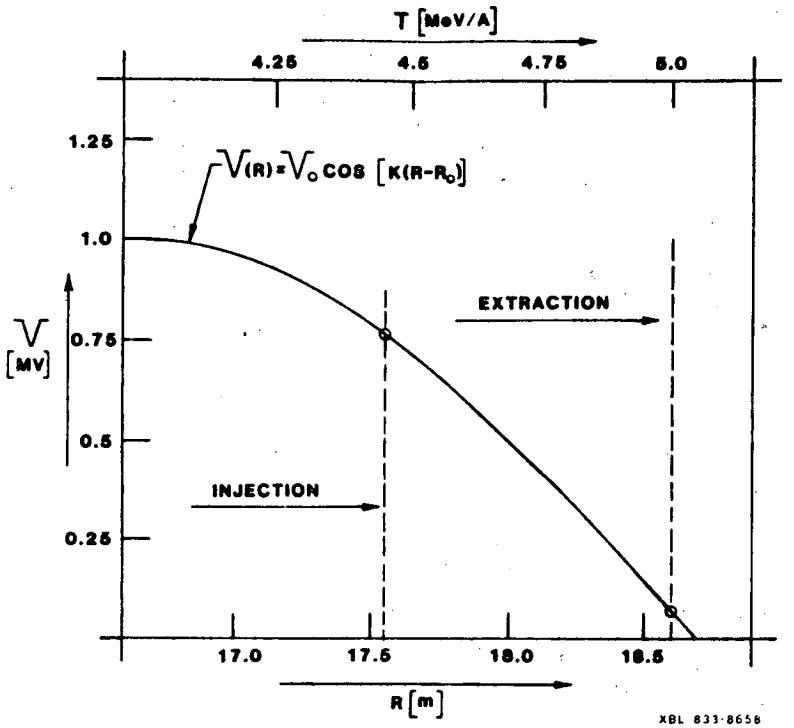

Fig. 1 - RF accelerating voltage as a function of radius, for the ISR calculations of this paper.

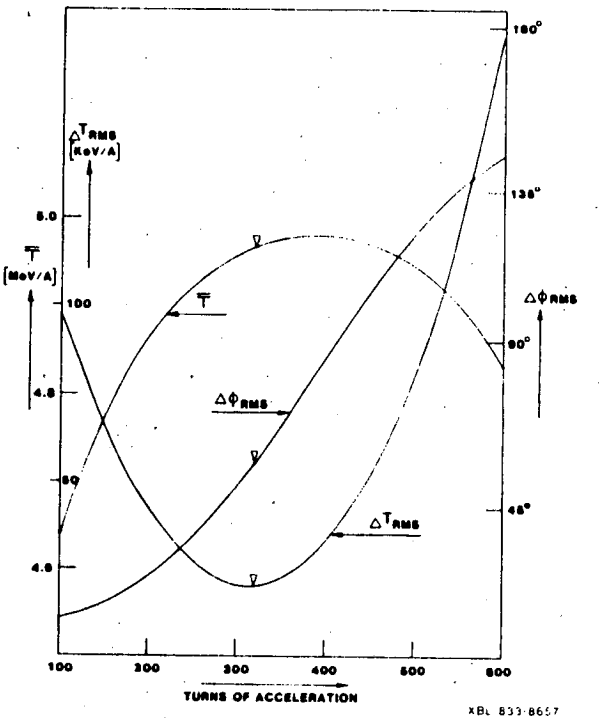

Fig. 2 - For a group of particles comprising 100 consecutive turns, the average energy $\bar{T}$, rms energy spread Δ rms, and rms phase spread $\Delta\Psi_{rms}$ are plotted, as a function of total accelerated turns. The triangles indicate the optimum point for extraction, after 320 turns.

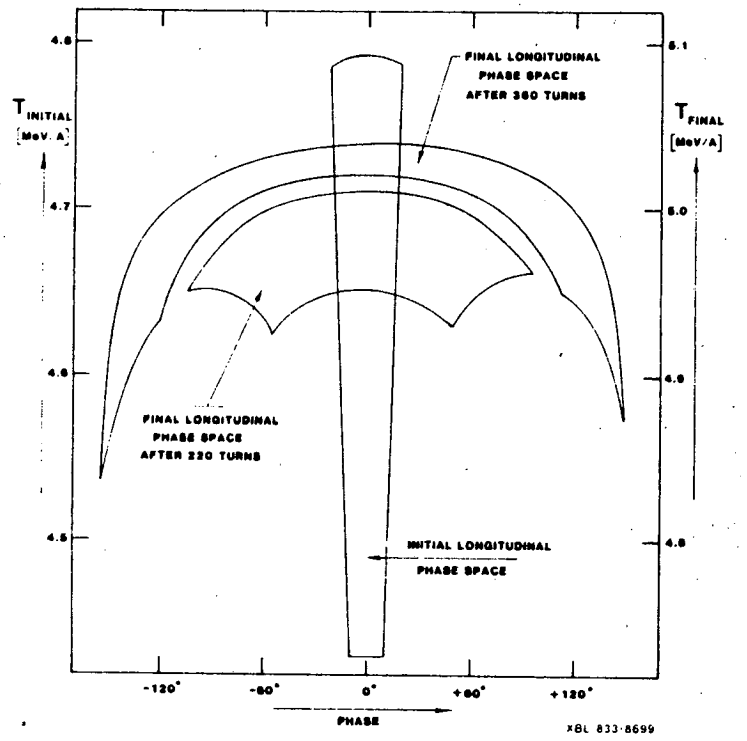

Fig. 3 - Distributions of 100 turns in ΔT, $\Delta\Psi$ phase space following turns 1, 220 and 360, showing the increasing distortion due to phase spreading.

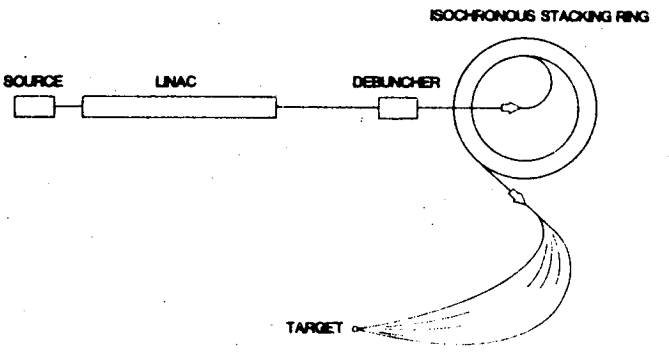

Fig. 4 - Schematic of a possible use of an isochronous stacking ring for the HTE.

Fig. 5 - Heating of a disk target by an ion beam. T_f is the asymptotic limit, where radiation and plasma losses equal heat input. The characteristic time τ is defined in the text.

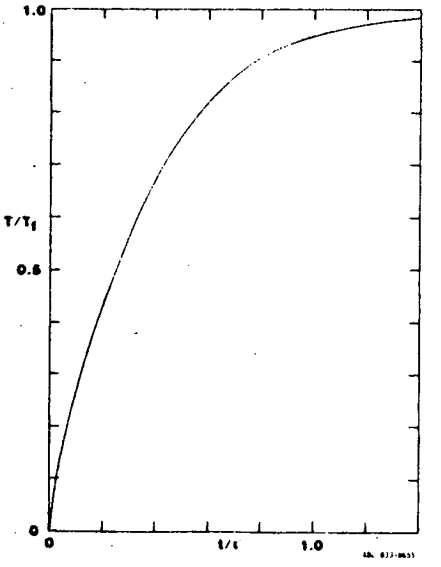

PUBLICATIONS

HI-FAN-204 (LBL-14922)	I. Hofmann L.J. Laslett L. Smith I. Haber	Stability of the KAPCHINSKIJ-VLADIMIRSKIJ (K-V) Distribution in Long Periodic Transport Systems (10/25/82)
HI-FAN-205	L.J. Laslett	Letters to Prof. M. Reiser Concerning Envelope Modes and 3rd-Order Modes in Periodic Transport Channels with $\sigma_o > 90^\circ$ (November 10, 1982)
HI-FAN-206 (LBID-646)	E. Lee	Plasma Phenomenon in AIF (Oct. 5, 1982)
HI-FAN-207 LBL-15233	Denis Keefe	"The Challenge of Ultra-High Energies-- Ultimate Limits, Possible Directions of Technology, An Approach to Collective Acceleration" Presented during the Panel Discussion at the ECRA-RAL Meeting, "The Challenge of Ultra-High Energies", Oxford England, September 27-30, 1982
HI-FAN-208 (LBL-15123) UC-21	H.I.F. Staff	Heavy Ion Fusion Year-End Report October 1982
HI-FAN 209	L.J. Laslett	Letter to Dr. I. Haber (NRL) with Data Concerning Hard-Edge Interrupted Solenoid Transport Systems with Small Occupancy Factor (01/17/83)
HI-FAN-210	L.J. Laslett	Comments Concerning a 3rd Order Canonical Integration Algorithm Developed by R. Ruth. (1/83)
HI-FAN-211 LBL-14487	Kenneth Reed Stalder (Ph.D. thesis)	$Cs^+ + Cs^+$ Charge Transfer and Ionization Cross Section Measurements by a Plasma Target Technique (01/26/83)
HI-FAN-212	L.J. Laslett	Introduction of Space Charge (for a K-V distribution) 01/26/83
HI-FAN-213	L.J. Laslett	Concerning Limits to the Acceptable Aperture Ratio in Periodic Electrostatic Quadrupole/Transport Channels-- A Preliminary Account-- 1/26/83
HI-FAN-214	L.J. Laslett	Letter to Pro. Reiser, Concerning X-Y Transverse Modes in the G.S.I. Experimental Transport Lattice (2/28/83).

HI-FAN-215 LBL-14416	M. Lampel M. Tiefenback	Elimination of Current Transients in a One-Dimensional Heavy-ion Diode (1/83)
HI-FAN-216 LBL-15119	A. Faltens et al.	Long-Pulse Induction Acceleration of Heavy-Ions, to be published in the Proceedings of the 1983 Particle Accelerator Conference (4/83)
HI-FAN-217 LBL-15117	J. Bisognano I. Haber L. Smith	Threshold Behavior for Longitudinal Stability of Induction Linac Bunches, to be published in the Proceedings of the 1983 Particle Accelerator Conference (4/83)
HI-FAN-218 LBL-15132	W. Chupp et al.	A Quadrupole Beam Transport Experiment for Heavy Ions under Extreme Space Charge Conditions, to be published in the Proceedings of the 1983 Particle Accelerator Conference (4/83)
HI-FAN-219 LBL-15208	F. Selph H. Grunder B. Leemann	An Isochronous Stacking Ring Approach to the HTE to be published in the Proceedings of the 1983 Particle Accelerator Conference (4/83)

HEAVY ION FUSION ROSTER

Denis Keefe

Warren W. Chupp
Edwin R. Edwards
Andris Faltens
Milton Firth
Edward C. Hartwig
Charles H. Kim
Michael Lampel
Edward J. Lofgren
Ross G. Nemetz
Chester D. Pike
Stephen S. Rosenblum
Gerald L. Stoker
Michael Tiefenback
David Vanecek

Theory

Lloyd Smith

Joseph Bisognano
Victor Brady
Alper A. Garren
Geoffrey Krafft
L. Jackson Laslett

William B. Hermannsfeldt, SLAC

HALF-YEAR REPORTS: Master Distribution List

Argonne National Lab.

Thomas A. Fields
Ronald Martin

University of Arizona

R. Morse

Batelle

John Hartman

Bechtel

W. Allen

Brookhaven National Lab.

Mark Barton
Alfred Maschke

C.E.A. Bruyeres-le-Chatel

R. Dei-Cas

University of Calif., Irvine

Norman Rostoker

University of Calif., Riverside

Robert Poe

Cornell University

John Nation
Ravi N. Sudan

DARPA

Richard Gullickson
Joe Mangano

Department of Energy

DP

S. Barish
John Freeman
Terry Godlove
Sheldon L. Kahalas
L. Killion
G. Kuswa
H. Roser, Asst. Sec., Defense Programs
R. Schriever

ER

James S. Kane
Richard Kropschot
James Leiss
Gerry Peters
David F. Sutter
Alvin Trivelpiece, Dir., Office of Energy Research
William Wallenmeyer

DoE San Office

Rudolf Bredderman
Z. Zafiris

E.P.R.I.

Ken Billman

Fermi National Accelerator Lab.

Frank T. Cole
Fred Mills
Lee Teng

GANIL

P. Lapostolle

GSI

R. Bock
D. Boehne

University of Illinois

G. Miley
Joseph Verdeyen

KMS Fusion, Inc.

Alex Glass
Henry J. Gomberg

Kanazawa University

S. Kawasaki

Lawrence Berkeley Laboratory

Bob Avery
Joseph Bisognano
Warren Chupp
Tom Elioff, 46C
Andy Faltens
Al Garren
Hermann Grunder, 50/149
Ed Hartwig
Egon Hoyer
Earl Hyde, 50A/4133E
Rob Johnson, 50/149
Dave Judd
Denis Keefe
Charles Kim
John Knight, 62/203
Wulf Kunkel, 4/230
Glen Lambertson
L. Jackson Laslett
Ed Lee
Edward Lofgren
Jack Peterson
Stephen Rosenblum
Andrew Sessler, 4/230
Bill Shanahan, 50C/001
David Shirley, 50A/4113
Lloyd Smith

Lawrence Livermore Laboratory

Richard J. Briggs, L-321
John L. Emmett, L-488
William Krupke, L-488
Jim Mark, L-477
Michael J. Monsler, L-481
John Nuckolls, L-477

Los Alamos National Laboratory

Roger Bangerter
Ihor Bohachevsky
Richard Cooper
Robert Jameson
Don Kerr
A. Peaslee
Roger B. Perkins
Steve Rockwood
George Sawyer
Richard Stokes
Don Swenson

University of Maryland

Martin Reiser
Derek Tidman

Max Planck Inst. fur Plasma Physik Garching

Ingo Hofmann

Maxwell Laboratories

Library

National Bureau of Standards

S. Penner
M. Wilson

National Science Foundation

Edward Knapp, Director

Naval Research Lab.

Steven Bodner
T. Coffey
Irving Haber
Philip Sprangle
Peter Turchi

Occidental Research Corp.

Wyn Salisbury

Physics International

Library

RAFAEL

Joseph Shiloh

Rutherford Laboratory

John D. Lawson
Chris Pryor

Sandia Laboratories

Everet H. Beckner
Don Cook
Tom Martin
J.P. Vandevender
Gerold Yonas

Soka University

Tetsuya Saito

SOREQ Nuclear Research Center

A. Sternlieb

SLAC

William Herrmannsfeldt
W. K. H. Panofsky
Burton Richter

TRW

J. Gordon
Z. Guiragossian
J. Maniscalco

Westinghouse

E. W. Sucov

University of Wisconsin

G. Kulcinski
G. Moses
R. Peterson

This report was done with support from the Department of Energy. Any conclusions or opinions expressed in this report represent solely those of the author(s) and not necessarily those of The Regents of the University of California, the Lawrence Berkeley Laboratory or the Department of Energy.

Reference to a company or product name does not imply approval or recommendation of the product by the University of California or the U.S. Department of Energy to the exclusion of others that may be suitable.

TECHNICAL INFORMATION DEPARTMENT
LAWRENCE BERKELEY LABORATORY
UNIVERSITY OF CALIFORNIA
BERKELEY, CALIFORNIA 94720